University of Central Lancashire UCLan

# Central Lancashire Online Knowledge (CLoK)

| | |
|---|---|
| Title | Magnetic excitations of the charge stripe electrons below half doping in La2−xSrxNiO4 (x = 0.45, 0.4) |
| Type | Article |
| URL | https://clok.uclan.ac.uk/13966/ |
| DOI | ##doi## |
| Date | 2017 |
| Citation | Freeman, Paul Gregory orcid iconORCID: 0000-0002-5376-8940, Giblin, S R, Hradil, K, Mole, R A, Cermak, P and Prabhakaran, D (2017) Magnetic excitations of the charge stripe electrons below half doping in La2−xSrxNiO4 (x = 0.45, 0.4). Physical Review B, 95 (6). 064403. ISSN 2469-9950 |
| Creators | Freeman, Paul Gregory, Giblin, S R, Hradil, K, Mole, R A, Cermak, P and Prabhakaran, D |

It is advisable to refer to the publisher's version if you intend to cite from the work. ##doi##

For information about Research at UCLan please go to http://www.uclan.ac.uk/research/

All outputs in CLoK are protected by Intellectual Property Rights law, including Copyright law. Copyright, IPR and Moral Rights for the works on this site are retained by the individual authors and/or other copyright owners. Terms and conditions for use of this material are defined in the http://clok.uclan.ac.uk/policies/

# Magnetic excitations of the charge stripe electrons below half doping in $La_{2-x}Sr_xNiO_4$ ($x = 0.45, 0.4$)

P. G. Freeman,[1,2,3,4,*] S. R. Giblin,[5,6] K. Hradil,[7,8] R. A. Mole,[9,10] P. Cermak,[11] and D. Prabhakaran[12]

[1]*Jeremiah Horrocks Institute for Mathematics, Physics, and Astronomy, University of Central Lancashire, Preston, PR1 2HE, United Kingdom*
[2]*Laboratory for Quantum Magnetism, Ecole Polytechnique Fédérale de Lausanne (EPFL), CH/1015 Lausanne, Switzerland*
[3]*Helmholtz-Zentrum Berlin, Hahn-Meitner-Platz 1, 14109 Berlin, Germany*
[4]*Institute Laue-Langevin, 71 avenue des Martyrs, CS 20156, 38042 Grenoble CedeX 9, France*
[5]*ISIS Facility, Rutherford Appleton Laboratory, Chilton, Didcot, Oxon, OX11 0QX, United Kingdom*
[6]*School of Physics and Astronomy, Queens Building, The Parade, Cardiff University, CF24 3AA, United Kingdom*
[7]*Institut für Physikalische Chemie, Universität Göttingen, Tammanstrasse 6, 37077 Göttingen, Germany*
[8]*T.U Wien, X-ray Centre, Getreidemarkt 9, A-1060 Vienna, Austria*
[9]*Forschungs-Netutronquelle Heinz Maier-Leibnitz (FRM II), Lichtenbergstraße, 1 85747 Garching, Germany*
[10]*Bragg Institute, ANSTO, New Illawarra Road, Lucas Heights, NSW, Australia*
[11]*Jülich Centre for Neutron Science at Heinz Maier-Leibnitz Zentrum (MLZ), Forschungszentrum Jülich GmbH, Lichtenbergstraße, 1 85748 Garching, Germany*
[12]*Department of Physics, Oxford University, Oxford, OX1 3PU, United Kingdom*

(Received 19 November 2015; revised manuscript received 28 December 2016; published 3 February 2017)

The low energy magnetic excitation spectrum of charge stripe ordered $La_{2-x}Sr_xNiO_4$, $x = 0.4$ and $x = 0.45$ samples, were studied by neutron scattering. Two excitation modes are observed in both materials, one from the ordered magnetic moments, and a second mode consistent with pseudo-one-dimensional antiferromagnetic excitations of the charge stripe electrons (q-1D). The dispersion of the q-1D excitation follows the same relation as in $x = 1/3$ composition, with even spectral weight in the two counterpropagating branches of the $x = 0.4$ sample, however in the $x = 0.45$ sample only one dispersion branch has any measurable spectral weight. The evolution of the q-1D excitations on doping to the checkerboard charge ordered phase is discussed.

DOI: 10.1103/PhysRevB.95.064403

Variation between the hourglass shaped magnetic excitation spectrum of the cuprates compared to the magnetic excitations of charge stripe ordered $La_{2-x}Sr_xNiO_{4+\delta}$ (LSNO) has called into question the relevance of the charge stripe picture for the cuprates [1–5]. Recently however, it has been shown that insulating charge stripe ordered $La_{5/3}Sr_{1/3}CoO_{4+\delta}$ (LSCoO) has an hourglass shaped magnetic excitation spectrum that can be explained within a similar linear spin wave model used to describe charge stripe ordered LSNO [6]. In the charge stripe model the reason behind the different excitation spectrums is in part due to disorder, but mainly due to the relative strength of the interstripe magnetic interaction across the charge stripe, relative to the the intrastripe interaction [6]. For a weak interstripe interaction an hourglass excitation is observed, whereas a strong interaction leads to the symmetric spin wave cones observed in LSNO [3,5]. The role of disorder in wiping out the mode that disperses away from the antiferromagnetic position has been established in a charge stripe ordered manganate, these modes are present at base temperature but they have no measurable intensity on warming to the magnetic ordering temperature [7]. In the case of $La_{2-x}Sr_xCoO_{4+\delta}$ an alternative scenario for the hourglass excitation spectrum arising from disordered checkerboard charge-ordered state has been proposed [8]. With the recent direct evidence of charge stripe order in $La_{2-x}Sr_xCoO_{4+\delta}$, the origin of the magnetic hourglass excitation spectrum is in dispute in this material [9].

In LSNO magnetic excitations of the charge stripe electrons are observed [10], whereas half-filled charge stripes in the cuprates appear to have no interunit cell spin interactions, and the spin state of the charge stripes in LSCoO is effectively $S = 0$ [1,2]. In the case of the cuprates there is evidence for a $\mathbf{Q} = 0$ intraunit cell magnetic order from certain experimental techniques [11], this is apparently affected by charge stripe order in La-based cuprates possibly indicating the involvement of spins of half-filled stripes [12]. It is necessary to understand the magnetic interactions of the charge stripe electrons in LSNO to throw light on how they mediate the strong interstripe spin interaction in these materials, which results in the spin wave cone dispersion of the magnetic excitations.

It has been shown in LSNO around $x \sim 1/3$ there are doping independent gapped quasi-one-dimensional antiferromagnetic correlations along the charge stripes of the $S = 1/2$ charge stripe electrons (q-1D) [10,13]. Where the periodicity of the order is four Ni sites long. Figure 1(a) shows the wave vector positions of magnetic excitations from the ordered $Ni^{2+}$ $S = 1$ and the magnetic excitations form the q-1D mode in LSNO. In the $x = 0.5$ the charge order is part stripe and part checkerboard in character. The q-1D excitation in the $x = 0.5$ was observed to lock into the wave vector of the ordered $Ni^{2+}$ $S = 1$ spins at $(h + 1/2 \pm \varepsilon/2, k + 1/2 \pm \varepsilon/2, l)$, $\varepsilon = 0.445$ positions in reciprocal space, as shown in Fig. 1 [14]. In LSNO $\varepsilon$ is known as the incommensurability, where $1/\varepsilon$ is the average periodicity of the charge order. Further details of the low energy magnetic excitations of the $x = 0.50$ material, such as bandwidth and zone boundary of the q-1D excitation, remain unclear due to the broadening of magnetic excitations in comparison to the $x = 1/3$ material [14]. In this paper the issue of the q-1D excitation's lock in in the $x = 0.5$ composition is addressed by studying the striking difference of the q-1D excitation between $x = 1/3$ and $x = 0.5$ doping.

*pgfreeman@uclan.ac.uk

 ©2017 American Physical Society

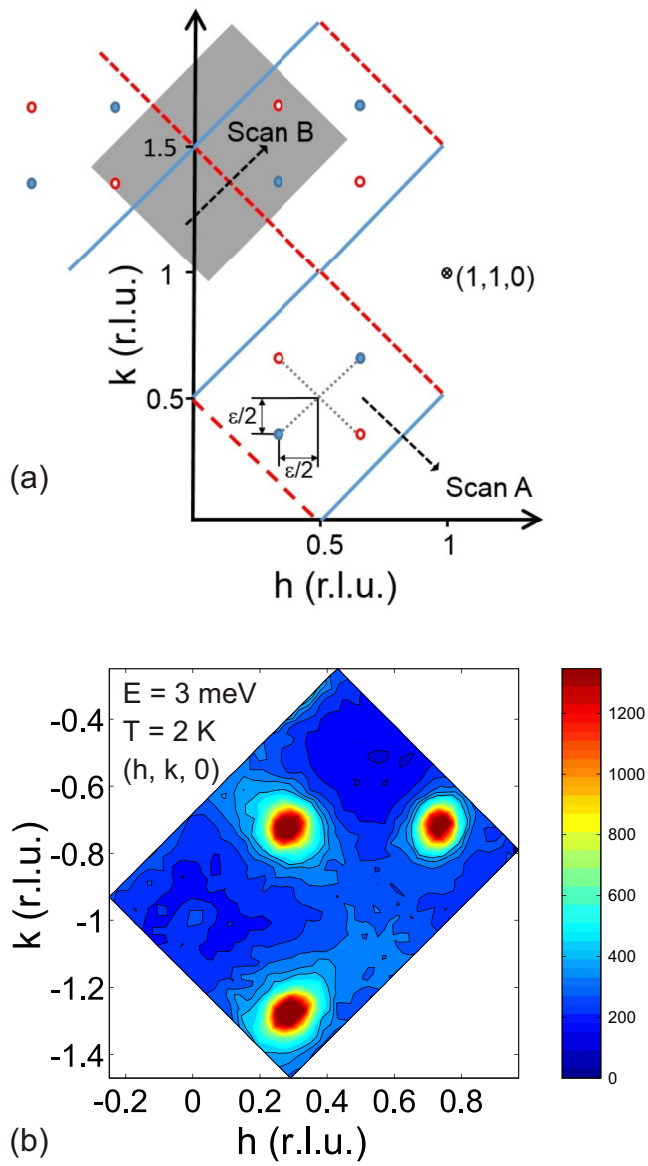


FIG. 1. (a) A diagram of the $(h,k,0)$ plane in reciprocal space for $La_{2-x}Sr_xNiO_{4+\delta}$. The location of magnetic Bragg reflections of the two spin stripe domains are represented by circles, and the (1,1,0) Bragg reflection is indicated. Dashed and solid lines indicate the location of gapped quasi-one-dimensional antiferromagnetic correlations of the charge stripe electrons (q-1D) at ≈1.5 meV. The filled circles and solid lines correspond to $[1,-1,0]$ charge stripe domains, and open circles and broken lines are for [1,1,0] stripe domains. The dotted arrows indicate the paths of two scans used to study the q-1D excitation in this paper, whereas the gray shaded rectangle is the approximate location of the grid scan used to study $La_{2-x}Sr_xNiO_4$ $x = 0.45$ at 3 meV shown in Fig. 3. (b) Low-energy scattering from $La_{3/2}Sr_{1/2}NiO_4$ measured by a grid of scans at 3 meV. The three centers of scattering are from excitations from the spin stripe ordered $Ni^{2+}$ spins, and the extended ridges underneath these excitations are from quasi-one-dimensional antiferromagnetic excitations of the charge stripe electrons. The existence of two modes was confirmed by the temperature dependencies of the excitations [14].

Single crystals of $La_{2-x}Sr_xNiO_4$ $x = 0.4$ and $x = 0.45$ compositions were grown using the floating-zone technique [15]. The $x = 0.4$ sample was a slab of dimensions $\approx 15 \times 10 \times 4$ mm and weighs 1.8 g. The $x = 0.45$ sample investigated was a rod of 6 mm in diameter and 25 mm in length weighing 2.5 g. The samples used here are the same samples that were studied in previous neutron diffraction measurements [16,17]. Oxygen content of as grown $x = 0.4$ sample was determined to be stoichiometric by thermogravimetric analysis [15], and the results of the neutron diffraction study of $x = 0.45$ sample are consistent with stoichiometric oxygen content [17,18]. The bulk magnetization of the $x = 0.45$ sample is found to have the same characteristics as a slightly oxygen deficient $x = 0.5$ sample, but the $x = 0.45$ sample has the advantage of being well removed from the checkerboard charge ordered state [17,19,20].

Neutron scattering experiments were performed on the triple-axis spectrometers PUMA [21] and PANDA [22] at the Heinz-Maier Leibnitz Zentrum, and IN8 at the Institut Laue-Langevin [23]. The data were collected with a fixed final neutron wave vector of $k_f = 2.662$ Å on PUMA and IN8, and $k_f = 1.55$ Å on PANDA. On PUMA and IN8 a pyrolytic graphite (PG) filter, and on PANDA a Beryllium filter, was placed after the sample to suppress higher-order harmonic scattering. The excitation spectrum of the $x = 0.45$ sample was measured on PUMA and PANDA, and the excitation spectrum of the $x = 0.4$ sample was measured on IN8. On all instruments the neutrons final and initial energy was selected by Bragg reflection off a double focusing pyrolytic graphite (PG) monochromator and double focusing analyzer (PUMA and IN8 and PANDA). The sample was orientated so that on all instruments $(h, k, 0)$ positions in reciprocal space could be accessed. In this work the tetragonal unit cell of LSNO is referred to, with unit cell parameters $a \approx 3.8$ Å, $c \approx 12.7$ Å. A report on the magnetic excitation spectrum from the ordered $Ni^{2+}$ spins has been reported elsewhere [24], with the excitation spectrum extending to >50 meV.

In the energy range of this study there is little development of the dispersion of magnetic excitations from the $S = 1$ $Ni^{2+}$ spins, with inelastic neutron scattering unable to resolve the counterpropagating modes. In Fig. 2(a) an energy scan of the magnetic excitations of the $x = 0.4$ sample at the magnetic zone center with $\varepsilon = 0.37$ is shown. With increasing energy transfer the intensity is approximately constant before increasing in between 4 and 5.5 meV, then decreasing in intensity monotonically above 7 meV. The inset of Fig. 2(a) shows that a similar behavior is observed for the $x = 0.45$ sample at the magnetic zone center with $\varepsilon = 0.42$. For the $x = 1/3$ material and the $x = 0.5$ material polarized neutron scattering determined that this increase in intensity at low energy transfer is due to overcoming the out-of-plane anisotropy gap in LSNO, which is greatly reduced compared to the parent material [14,26]. We therefore assume that the increase intensity observed at similar energies in other doping levels is the out-of-plane anisotropy, including here for the $x = 0.4$ and $x = 0.45$ samples. In Fig. 2(b) the doping dependence of the assumed out-of-plane anisotropy gap is shown, with the anisotropy gap energy defined to be the lowest energy at which maximum intensity occurs. We note that the reduction in the out-of-plane anisotropy gap of charge stripe

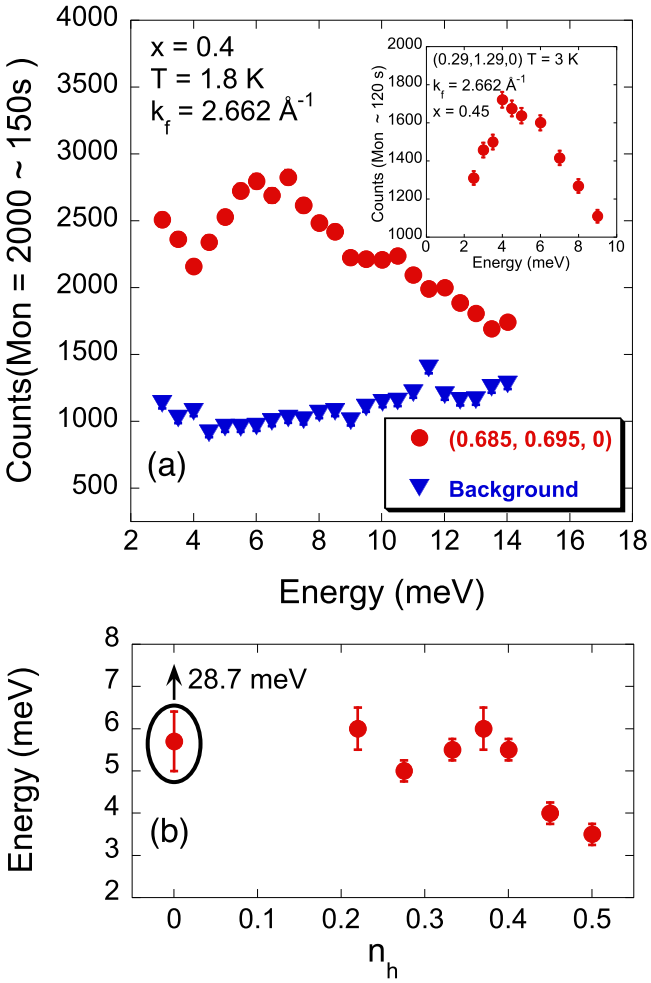


FIG. 2. (a) An energy scan of the magnetic excitations at the magnetic zone center of $La_{2-x}Sr_xNiO_4$, $x = 0.4$ sample. The background was measured at a wave vector $\pm(0.15,0.15,0)$ stepped away from the magnetic zone center, sufficiently spaced to avoid the q-1D excitation. Inset: An energy scan of the magnetic excitations at the magnetic zone center of $x = 0.45$ sample. In both energy scans the magnetic intensity first increases as the out-of-plane anisotropy gap is overcome, then decreases with increasing energy transfer as expected for antiferromagnetic excitations. (b) The doping variation of the out-of-plane anisotropy gap of $La_{2-x}Sr_xNiO_{4+\delta}$, where $n_h = x + 2\delta$, is the hole concentration. Additional data points taken from previous studies [5,14,25–27].

ordered LSNO is similar to that reported for $La_{2-x}Sr_xCuO_4$ [28].

In previous studies it has been demonstrated that an effective way to determine the location of the q-1D excitation is to map out reciprocal space in a grid scan at a fixed energy transfer [10,14]. In Fig. 3 a grid scan of the excitations of the $x = 0.45$ sample at 3 meV measured at 3.5 K is shown. White circles have been added to this figure to indicate the magnetic zone centers of the ordered $Ni^{2+}$ spins, where intense magnetic excitations are observed to be dispersing out of the magnetic zone centers. Additional to the zone center magnetic excitations, diffuse ridges of scattering are present that are consistent with the presence of q-1D correlations [10,13,14].

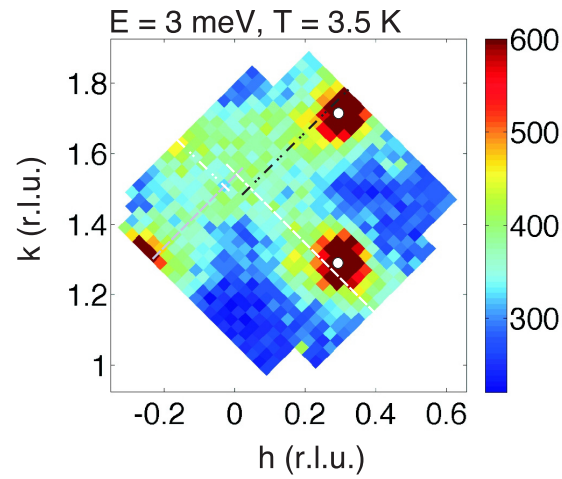


FIG. 3. A grid of low energy neutron scans on the $x = 0.45$ sample performed at 3 meV, performed on PUMA. White circles indicate the wave vector of Bragg reflections from the spin stripe ordered $Ni^{2+}$ spins, while the four dashed lines are guides to the eye of the four diffuse ridges of scattering observed in this grid scan.

By performing scans parallel to the q-1D excitations that pass through the excitations of the ordered $Ni^{2+}$ spins, we can determine a position where there is zero intensity from the excitations from the ordered spins. At this position scans across the q-1D excitations can be performed to map out the dispersion of the q-1D scattering. Figure 4 shows constant energy scans across the q-1D excitations for the (a) $x = 0.4$ sample and (b) $x = 0.45$ sample. In the $x = 0.4$ sample the constant energy scans are well described by fitting two Gaussian line shapes on a sloping background, with the splitting of the two peaks increasing with increasing energy transfer. Figure 4(b) however shows that in the $x = 0.45$ sample the dispersion of the q-1D excitations can be fitted by one Gaussian line shape on a sloping background that disperses with increasing energy transfer. There is a small shoulder of scattering on the left-hand side of the 9 meV peak that is not perfectly described by this line shape, and there maybe a relatively weak excitation mode. The dispersion of the q-1D excitations is clearly different in the two doping levels studied here, in the $x = 0.4$ sample there are two counterpropgating modes, whereas in the the $x = 0.45$ sample only one dispersive mode is observed to have significant spectral weight.

Further measurements of the q-1D excitations have been performed on the $x = 0.45$ sample to lower energies using the higher energy resolution of the cold triple axis spectrometer PANDA with $k_f = 1.55$ Å. In Fig. 5 constant energy scans of the $x = 0.45$ sample at 1.0, 1.5. and 2 meV are fitted by a Gaussian line shape on a sloping background. The scan of the q-1D excitations at 1.0 and at 1.5 meV are significantly broadened compared to the scan at 2.0 meV. Calculations of the resolution ellipsoid of the experimental setup indicate this broadening is not due to focusing and defocusing effects, the broadening is intrinsic to the q-1D excitations. At 2.0 and 1.5 meV the peak centers are consistent with a $\xi = 0.25$ centering of the q-1D. In comparison to the intensity of q-1D excitations at 2.0 and 1.5 meV there is an apparent $64 \pm 32\%$ increase in intensity observed at 1.0 meV. Attempts to measure

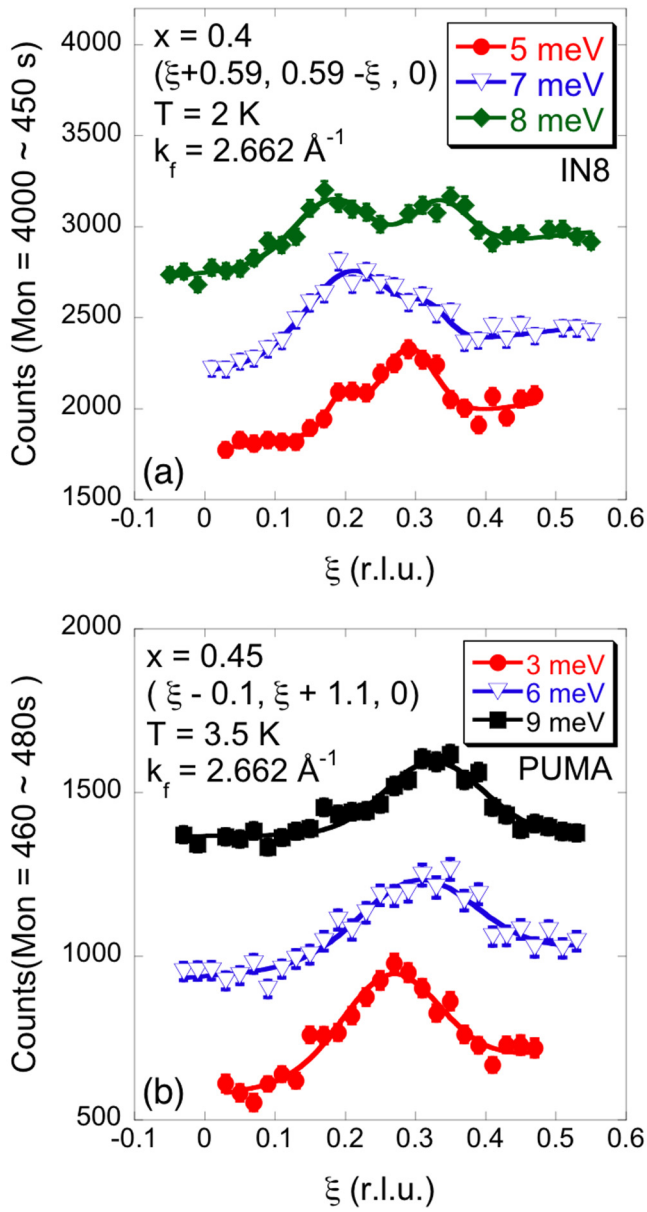


FIG. 4. Constant-energy scans across the q-1D excitation, for (a) the $x = 0.4$ sample (scan A) and (b) the $x = 0.45$ sample (scan B). Successive scans have been offset vertically by the addition of (a) 500 counts and (b) 250 counts, for the purpose of clarity. The solid lines are the result of a fit to the data of a sloping background with (a) two Gaussian line shape and (b) one Gaussian line shape.

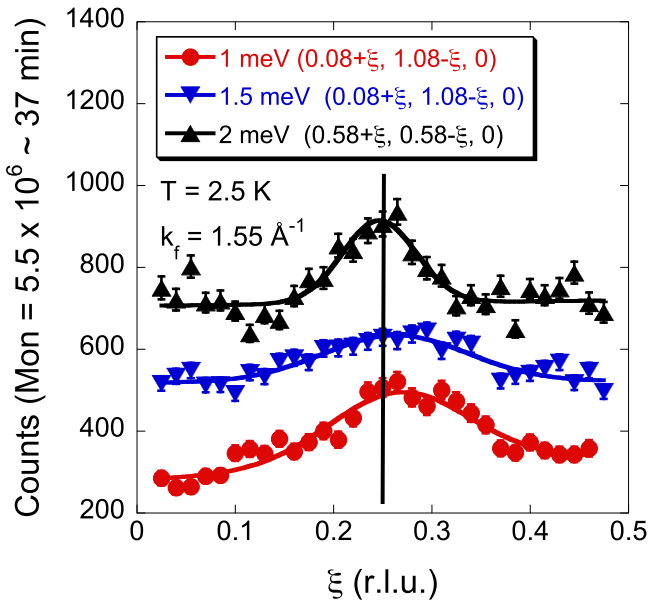


FIG. 5. Constant-energy scans across the q-1D excitation in the $x = 0.45$ sample measured at 1.0, 1.5 (scan B), and 2 meV (scan A). The solid lines are the result of a fit to the data of a sloping background with one Gaussian line shape. The wave vector resolution parallel to the scan resolution is 0.0124 r.l.u. at 1.0 meV, 0.0127 r.l.u. at 1.5 meV, and 0.0131 r.l.u. at 2 meV. A broadening of the q-1D excitation is observed in scans at 1.0 and 1.5 meV, compared to 2 meV.

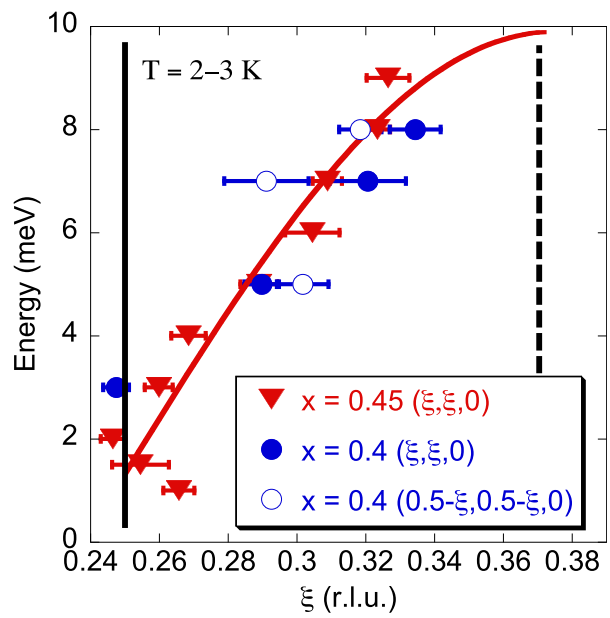


FIG. 6. The fitted centers of the q-1D excitations obtained from constant energy scans such as those shown in Figs. 4 and 5. A solid vertical line represents the zone center, and a dashed vertical line represents the zone boundary of the q-1D excitation. Centers of the q-1D excitation at 5, 7, and 8 meV in the $x = 0.4$ that disperse to smaller values of $\xi$ have been folded into this half Brillouin zone for better comparison with the dispersion of the $x = 0.45$ sample. The $x = 0.45$ sample data are fitted with a gapped sinusoidal dispersion for the expected q-1D excitation periodicity, with the fit being consistent with the dispersion of the q-1D excitation observed in the $x = 1/3$ material [10,13].

the energy gap in a higher resolution mode with $k_f = 1.2$ Å suffered from low count rates.

To compare the dispersion of the q-1D excitations in the $x = 0.45$ and $x = 0.4$ samples the energy variation of the fitted peak centers obtained in constant energy scans is shown in Fig. 6. The centers of the q-1D excitations in the $x = 0.4$ sample have been folded into a half Brillouin zone for comparison purposes. Within the experimental error there is no significant difference in the dispersion of the q-1D excitations of the $x = 0.45$ and $x = 0.4$ samples, indicating the main interactions of the q-1D excitations are the same in both materials.

In the $x = 1/3$ the dispersion of the q-1D excitations was originally compared to a Heisenberg spin-1/2 antiferromagnet spin chain, before the spin gap was determined [10]. We therefore compare the $x = 0.45$ sample dispersion of Fig. 4 to that of a Heisenberg spin-1/2 antiferromagnet spin chain with the inclusion of a gap term:

$$E(\mathbf{Q}) = \mathbf{E_0} + \pi \mathbf{J}|\mathbf{sin}(2\pi \mathbf{Q}.\mathbf{d})|, \quad (1)$$

where $E_0$ is the spin gap, $J$ is the nearest neighbor exchange interaction per spin, and $\mathbf{d} = [1,1,0]$ is the direction parallel to the charge stripes. From this fit we obtain an energy gap $E_0 = 1.3 \pm 0.5$ meV and a spin exchange interaction per spin of $J = 2.7 \pm 0.3$ meV. In the $x = 1/3$ material the energy width of the q-1D excitations was determined by scanning the zone center excitations to be $1.57 \pm 0.17$ meV, indicating the excitations are short lived [13]. If the q-1D excitations in the $x = 0.45$ sample had a 1.6 meV energy width, this would explain why the q-1D excitations are observed at 1 meV in the $x = 0.45$ sample. The wave vector of the q-1D excitation indicates a four spin object, this object may better map onto a one-dimensional Haldane spin chain of integer spins, with a Haldane spin chain having a spin gap and bandwidth of $4J$ instead of $\pi J$ for a Heisenberg spin-1/2 antiferromagnet spin chain [29]. The recent development of polarized neutron scattering for time-of-flight inelastic spectrometers would provide the ability to separate phonon and magnetic scattering enabling mapping of the magnetic excitations in the 10–20 meV energy range [30], this would enable measurements to determine if the q-1D has continuum of excitations to differentiate between these two situations. Surprisingly the parameters obtained from this phenomenological fit accurately describe the dispersion of the q-1D excitation of the $x = 1/3$ [10,13], further showing the doping independence of the main spin interaction of the q-1D excitations.

Charge stripes in LSNO have been determined to be predominantly centered on Ni sites at low temperature [31], so that between a 1/3 and 1/2 doping the charge stripe structure is believed to be an admixture of the $\varepsilon = 0.5$ and $\varepsilon = 1/3$ structures [18]. As the doping level is increased towards 1/2 doping, the charge stripe structure becomes closer to the $\varepsilon = 0.5$ of ideal checkerboard charge order. In checkerboard charge order there is simultaneously charge order at 45° to the Ni-O bonds along both diagonal directions of the Ni-O plane. Previously it has been shown that the charge stripe structure is determined predominantly by the Coulomb interaction between the charge stripe electrons [31]. The distortion of the lattice by the charge stripe order is what enables neutron diffraction to study the charge stripe order. On going towards the checkerboard charge ordered phase the charge order loses itÕs definition, effectively having zero correlation length out of the Ni-O planes at 1/2 doping [18,20]. With a reduction in the distortion of the lattice caused by charge order, different pathways for magnetic interactions may therefore be enabled, or enhanced.

For Ni centered charge stripe order with $\varepsilon > 0.418 = (0.5 + 0.333)/2$, on average a charge stripe will have one neighboring charge stripe two Ni-Ni spacings apart as in checkerboard charge order, and another charge stripe neighbor three Ni-Ni spacings apart. For the two Ni-Ni spaced charge stripes there is locally a checkerboard structure, so the charge stripe electrons will want to interact antiferromagnetically at right angles to the charge stripe direction. The charge order at right angles to the charge stripe direction is however too short for the four Ni spin object of the q-1D excitation to form, nevermind propagate, so an intercharge stripe spin interaction will be limited to a perturbation of the q-1D excitation. Below $\varepsilon = 0.418$ there will be charge stripes that have two neighboring charge stripes three Ni-Ni spacings apart, leading to a well-defined stripe direction, and what should be a stronger lattice distortion caused by the charge order that weakens any intercharge stripe spin interaction. We tentatively propose that the observed loss in spectral weight of the q-1D excitation dispersing away from the antiferromagnetic position in reciprocal space in the $x = 0.45$ sample is caused by a reduction in the charge-order distortion that enables a perturbing intercharge stripe antiferromagnetic interaction between charge stripes two Ni-Ni spacings apart.

In the cuprates and cobaltates it has been proposed that the hourglass magnetic excitation spectrum arises due a small ratio of interstripe to intrastripe magnetic interactions, and disorder of the spin interactions [6,7]. The intercharge stripe spin interaction, we tentatively propose for the loss in spectral weight of one mode of the q-1D excitation in the LSNO $x = 0.45$ material, has a similar role as disorder in producing an hourglass shaped excitation spectrum. We note that the alternative nanophased separated model of the cobaltates also includes disorder of the magnetic order [8].

The proposed cause of the change of the q-1D excitations $x = 0.45$ material compared to the $x = 0.4$ material is different to the change in the magnetic excitations from the ordered $S = 1$ $Ni^{2+}$ spin stripes in these two materials [24]. For the magnetic excitations from the ordered spins it was proposed that the variation in charge stripe periodicity caused damping of the magnetic excitations from the ordered spins below $\varepsilon = 0.418$, whereas as above $\varepsilon = 0.418$ variation in charge stripe periodicity is abrupt and causes additional magnetic excitation modes.

This study has shown the remarkable doping independence of the dispersion of q-1D magnetic excitations and their quasi-one-dimensionality in LSNO over the doping range $x = 0.275$ to $x = 0.45$. Despite the lack of variation in the dispersion of the q-1D scattering there is a dramatic loss of spectral weight in one dispersion branch on going from $x = 0.4$ to $x = 0.45$ hole doping as the stripe direction definition is reduced. This leads to an alternative explanation to a wave vector lock in of the q-1D to the ordering spin stripe wave vector in the $x = 0.5$, an accidental observation of co-incidence due to the softening of the dispersion of the q-1D excitations [14]. Further investigation of the dispersion relation of q-1D excitations in the $x = 0.5$ are warranted.

We wish to acknowledge that crystal growth for this work was supported by the Engineering and Physical Sciences Research Council of Great Britain. We wish to acknowledge that this research project has been supported by the European Commission under the 6th Framework Programme through the Key Action: Strengthening the European Research Area, Research Infrastructures. Contract No. RII3-CT-2003-505925.

[1] J. M. Tranquada, B. J. Sternleib, J. D. Axe, Y. Nakamura, and S. Uchida, Nature (London) **375**, 561 (1995).

[2] S. M. Hayden, H. A. Mook, P. Dai, T. G. Perring, and F. Doan, Nature (London) **429**, 531 (2004); J. M. Tranquada, H. Woo, T. G. Perring, H. Goka, G. D. Gu, G. Xu, M. Fujita, and K. Yamada, *ibid.* **429**, 534 (2004).

[3] A. T. Boothroyd, D. Prabhakaran, P. G. Freeman, S. J. S. Lister, M. Enderle, A. Hiess, and J. Kulda, Phys. Rev. B **67**, 100407(R) (2003).

[4] P. Bourges, Y. Sidis, M. Braden, K. Nakajima, and J. M. Tranquada, Phys. Rev. Lett. **90**, 147202 (2003).

[5] H. Woo, A. T. Boothroyd, K. Nakajima, T. G. Perring, C. D. Frost, P. G. Freeman, D. Prabhakaran, K. Yamada, and J. M. Tranquada, Phys. Rev. B **72**, 064437 (2005).

[6] A. T. Boothroyd, P. Babkevich, D. Prabhakaran, and P. G. Freeman, Nature (London) **471**, 341 (2011).

[7] H. Ulbrich, P. Steffens, D. Lamago, Y. Sidis, and M. Braden, Phys. Rev. Lett. **108**, 247209 (2012).

[8] Y. Drees, D. Lamago, A. Piovano, and A. C. Komarek, Nat. Commun. **4**, 2449 (2013); Y. Drees, Z. W. Li, A. Ricci, M. Rotter, W. Schmidt, D. Lamago, O. Sobolev, U. Rütt, O. Gutowski, M. Sprung, A. Piovano, J. P. Castellan, and A. C. Komarek, *ibid.* **5**, 5731 (2013).

[9] P. Babkevich, P. G. Freeman, D. Prabhakaran, and A. T. Boothroyd, Nat. Commun. **7**, 11632 (2016).

[10] A. T. Boothroyd, P. G. Freeman, D. Prabhakaran, A. Hiess, M. Enderle, J. Kulda, and F. Altorfer, Phys. Rev. Lett. **91**, 257201 (2003).

[11] B. Fauqué, Y. Sidis, V. Hinkov, S. Pailhès, C. T. Lin, X. Chaud, and P. Bourges, Phys. Rev. Lett. **96**, 197001 (2006); Y. Li, V. Balèdent, N. Baris, Y. Cho, B. Fauquè, Y. Sidis, G. Yu, X. Zhao, P. Bourges, and M. Greven, Nature (London) **455**, 372 (2008); H. A. Mook, Y. Sidis, B. Fauqué, V. Balédent, and P. Bourges, Phys. Rev. B **78**, 020506(R) (2008); Y. Li, V. Balèdent, N. Baris, Y. C. Cho, Y. Sidis, G. Yu, X. Zhao, and P. Bourges, and M. Greven, *ibid.* **84**, 224508 (2011); S. De Almeida-Didry, Y. Sidis, V. Balèdent, F. Giovannelli, I. Monot-Laffez, and P. Bourges, *ibid.* **86**, 020504(R) (2012); L. Mangin-Thro, Y. Sidis, A. Wildes, and P. Bourges, Nat. Commun. **6**, 7705 (2015).

[12] V. Baledent, B. Fauqué, Y. Sidis, N. B. Christensen, S. Pailhès, K. Conder, E. Pomjakushina, J. Mesot, and P. Bourges, Phys. Rev. Lett. **105**, 027004 (2010).

[13] P. G. Freeman, D. Prabhakaran, K. Nakajima, A. Stunault, M. Enderle, C. Niedermayer, C. D. Frost, K. Yamada, and A. T. Boothroyd, Phys. Rev. B **83**, 094414 (2011).

[14] P. G. Freeman, A. T. Boothroyd, D. Prabhakaran, C. D. Frost, M. Enderle, and A. Hiess, Phys. Rev. B **71**, 174412 (2005).

[15] D. Prabhakaran, P. Isla, and A. T. Boothroyd, J. Cryst. Growth **237**, 815 (2002).

[16] P. G. Freeman, A. T. Boothroyd, D. Prabhakaran, M. Enderle, and C. Niedermayer, Phys. Rev. B **70**, 024413 (2004).

[17] S. R. Giblin, P. G. Freeman, K. Hradil, D. Prabhakaran, and A. T. Boothroyd, Phys. Rev. B **78**, 184423 (2008).

[18] H. Yoshizawa, T. Kakeshita, R. Kajimoto, T. Tanabe, T. Katsufuji, and Y. Tokura, Phys. Rev. B **61**, R854 (2000).

[19] P. G. Freeman, S. R. Giblin, and D. Prabhakaran, J Supercond. Nov. Mag. **24**, 1149 (2011).

[20] R. Kajimoto, K. Ishizaka, H. Yoshizawa, and Y. Tokura, Phys Rev B **67**, 014511 (2003).

[21] Heinz-Maier Leibnitz Zentrum *et al.*, PUMA: Thermal three axes spectrometer, J. Large-Scale Res. Facilities **1**, A13 (2015).

[22] Heinz-Maier Leibnitz Zentrum *et al.*, PANDA: Cold three axes spectrometer, J. Large-Scale Res. Facilities **1**, A12 (2015).

[23] A. Heiss, M. Jiménez-Ruiz, P. Courtois, R. Currat, J. Kulda, and F. J. Bermejo, Physica B: Condens. Matter **385-386**, 1077 (2006).

[24] P. G. Freeman, S. R. Giblin, K. Hradil, R. A. Mole, and D. Prabhakaran, J. Kor. Phys. Soc. **62**, 1453 (2013).

[25] K. Nakajima, K. Yamada, S. Hosoya, T. Omata, and Y. Endoh, J. Phys. Soc. Jpn. **62**, 4438 (1993).

[26] A. T. Boothroyd, P. G. Freeman, D. Prabhakaran, M. Enderle, and J. Kulda, Physica B **345**, 1 (2004).

[27] P. G. Freeman, M. Enderle, S. M. Hayden, C. D. Frost, D. X. Yao, E. W. Carlson, D. Prabhakaran, and A. T. Boothroyd, Phys. Rev. B **80**, 144523 (2009).

[28] A. T. Rømer, J. Chang, N. B. Christensen, B. M. Andersen, K. Lefmann, L. Mähler, J. Gavilano, R. Gilardi, Ch. Niedermayer, H. M. Rønnow, A. Schneidewind, P. Link, M. Oda, M. Ido, N. Momono, and J. Mesot, Phys. Rev. B **87**, 144513 (2013).

[29] F. D. M. Haldane, Phys. Rev. Lett. **50**, 1153 (1983); I. Affleck and F. D. M. Haldane, Phys. Rev. B **36**, 5291 (1987).

[30] C. Y. Jiang, X. Tong, D. R. Brown, S. Chi, A. D. Christianson, B. J. Kadron, J. L. Robertson, and B. L. Winn, Rev. Sci. Instrum. **85**, 1 (2014); B. Winn, U. Filges, V. O. Garlea, M. Graves-Brook, M. Hagen, C. Jiang, M. Kenzelmann, L. Passell, S. M. Shapiro, X. Tong, and I. Zaliznyak, EPJ Web Conf. **83**, 03017 (2015); J. Voigt, H. Soltner, E. Babcock, Z. Salhi, R. R. Gainov, T. Brükel, and R. Aldus, *ibid.* **83**, 03016 (2015); T. Yokoo, K. Ohoyama, S. Itoh, K. Iwasa, N. Kaneko, J. Suzuki, M. Ohkawara, K. Aizawa, S. Tasaki, T. Ino, K. Taketani, S. Ishimoto, M. Takeda, T. Oku, H. Kira, K. Hayashi, H. Kimura and T. J. Sato, *ibid.* **83**, 03018 (2015).

[31] P. Wochner, J. M. Tranquada, D. J. Buttrey, and V. Sachan, Phys. Rev. B **57**, 1066 (1998).